JOURNAL OF MATERIALS SCIENCE **39** (2004) 6539–6549

Deformation, stress relaxation, and crystallization of lithium silicate glass fibers below the glass transition temperature

S. T. REIS, CHEOL-WOON KIM, R. K. BROW, C. S. RAY*
Ceramic Engineering Department and Graduate Center for Materials Research, University of Missouri-Rolla, Rolla, MO 65409, USA
E-mail: reis@umr.edu

The deformation and crystallization of $Li_2O{\cdot}2SiO_2$ and $Li_2O{\cdot}1.6SiO_2$ glass fibers subjected to a bending stress were measured as a function of time over the temperature range ~50 to ~150°C below the glass transition temperature (T_g). The glass fibers can be permanently deformed at temperatures about 100°C below T_g, and they crystallize significantly at temperatures close to, but below T_g, about 150°C lower than the onset temperature for crystallization for these glasses in the no-stress condition. The crystallization was found to occur only on the surface of the glass fibers with no detectable difference in the extent of crystallization in tensile and compressive stress regions. The relaxation mechanism for fiber deformation can be best described by a stretched exponential (Kohlrausch-Williams-Watt (KWW) approximation), rather than a single exponential model.

The activation energy for stress relaxation, E_s, for the glass fibers ranges between 175 and 195 kJ/mol, which is considerably smaller than the activation energy for viscous flow, E_η (~400 kJ/mol) near T_g for these glasses at normal, stress-free condition. It is suspected that a viscosity relaxation mechanism could be responsible for permanent deformation and crystallization of the glass fibers below T_g.

1. Introduction

Many glass forming melts of inorganic oxide compositions behave as non-Newtonian liquids such that the strain rate (rate of shear flow) response under an applied stress is non-linear [1–9]. An aspect of non-Newtonian behavior of glass melts is shear thinning, a decrease in viscosity with increasing shear stress, which should have a pronounced effect on the nucleation and crystal growth rates, and, hence, on the overall tendency for crystallization of a glass. A smaller crystallization tendency produces a better glass. According to classical theory for nucleation and crystal growth [10], both the nucleation rate (I) and crystal growth rate (U) at any temperature (T) for a glass are inversely proportional to its viscosity, η, at T. The overall crystallization (or, the volume fraction of crystallization, X) of a glass at T depends jointly on I and U as,

$$X \propto I(T)U^3(T)t^4 \propto \left(\frac{t}{\eta}\right)^4 \qquad (1)$$

where, t is the time spent at T.

In the classical theories of nucleation and crystal growth [1, 6, 7], the viscosity, η, is tacitly assumed to be equal to the Newtonian viscosity, η_0. It is now evident that this assumption does not adequately describe the rheology of inorganic glasses even under moderate shear fields [1–9]. A more realistic approach, therefore, would be to use an effective, non-Newtonian viscosity, η_{eff}, to reflect the actual processing conditions of a melt as encountered in many commercial glass manufacturing processes like pressing, blowing, extruding, and fiber drawing. Such high-shear glass manufacturing processes can decrease substantially the isothermal viscosity of the glass, thereby increasing its overall tendency for crystallization. As shown in Equation 1, a decrease in viscosity by an order of magnitude would increase the overall crystallization tendency by four orders of magnitude. Thus, knowledge of the effect of shear stress on crystallization in glasses is important not only for a fundamental understanding of the nucleation and crystal growth processes under a shear field, but also to improving the technology currently used for processing glasses.

It has been reported that fluoride and oxide (silicate) glass fibers subjected to bending stresses can be permanently deformed at temperatures well below their respective glass transition temperatures, T_g, [11, 12] and this might be a consequence of shear thinning under the bending stress. The activation energy for

*Currently on Leave at George C. Marshall Space Flight Center, National Aeronautics and Space Administration, Huntsville, AL 35812, USA.

stress relaxation (E_s) is an easily measurable parameter which can be obtained by monitoring the deformation of the glass fibers as a function of temperature at a fixed applied stress. Comparing the values of E_s with the activation energy for viscous flow, E_η, should provide insight as to how the glass fibers are permanently deformed below the glass transition temperature.

The objectives of the present research are to investigate whether shear thinning (1) enhances the crystallization behavior of a glass and (2) causes permanent deformation in glass fibers below their glass transition temperatures. A few reports that qualitatively indicate shear-induced crystallization of oxide melts are available in the literature. Certain phosphate glasses when subjected to high shear mixing or extrusion at temperatures about 100°C above T_g (but still below the crystallization temperature) were shown to crystallize [4, 5]. However, to the best of our knowledge, no direct measurement for the effect of shear stress on crystallization of glasses has been reported up to this time.

2. Experimenatal procedure

Glass fibers of two compositions in the lithium silicate system have been used in the present investigations. One glass, $Li_2O{\cdot}2SiO_2$, is frequently used as a model glass for investigating nucleation and crystal growth kinetics, and a large body of thermodynamic and kinetic parameters for nucleation and crystal growth are available for this glass. The other glass, $Li_2O{\cdot}1.6SiO_2$, contains a slightly higher amount of Li_2O, which should alter the crystallization behavior of the glass compared to that for the $Li_2O{\cdot}2SiO_2$.

2.1. Glass melting and preparation

Homogeneous mixtures of Li_2CO_3 and SiO_2 crystalline raw materials for $Li_2O{\cdot}2SiO_2$ (here after referred to as LS_2) or $Li_2O{\cdot}1.6SiO_2$ (here after referred to as $LS_{1.6}$) were melted in a platinum crucible at 1400°C for 2 h in air. The nominal mol% compositions for LS_2 and $LS_{1.6}$ are $33.3Li_2O$–$66.7SiO_2$ and $38Li_2O$–$62SiO_2$, respectively. The melt was stirred (homogenized) three times, at 30 min intervals, during melting using an alumina rod. The temperature of the melt was then (after 2 h) decreased to 1300°C and the melt was held at this temperature for another 30 min. The platinum crucible containing the melt was removed from the furnace and glass fibers were drawn by hand using an alumina bait rod. The glass fibers, which had a uniform diameter of 150 ± 5 μm over a length of at least 120 mm were selected for experiments.

If the melt became too thick (viscous) before a sufficient number of glass fibers were obtained, the crucible containing the melt was returned to the furnace (at 1300°C) for another 30 min and the procedure described above was repeated to draw more glass fibers. A few of the glass fibers were crushed and ground to powders, and analyzed by X-ray diffraction (XRD) to confirm their amorphous character. As-made glass fibers were also analyzed by scanning electron microscopy (SEM) interfaced with energy dispersive X-ray analysis (EDS) to detect any dissolution of alumina into the melt during stirring. No alumina, however, was detected in the glass. The diameter of the glass fibers was measured by a micrometer at 10 to 12 different locations along the length, and an averaged was recorded.

2.2. Heat treatment

2.2.1. Fiber deformation, stress relaxation, and crystallization

The heat treatment used for investigating fiber deformation and stress relaxation was as follows. A glass fiber (120 mm long) was held in a bending configuration by fixing the fiber ends in a refractory block, as shown in Fig. 1. The distance between the holes, R_0, was set at 25 mm. Under this condition, the tip of the bent glass fiber is subjected to a constant bending stress. Another fiber of the same glass was held straight in the vertical direction approximately at the middle of the refractory block (Fig. 1), so that its top end extends up to the tip of the bent fiber. This straight fiber, which was under no stress, was used as a control sample.

The refractory block holding the bent and straight fibers was inserted into an annealing furnace previously set at a desired temperature, T. After heating for a specific time, t, the glass fibers were removed from the furnace. The bent fiber was released from the holes, and allowed to take its free and relaxed form as it cooled to room temperature. The separation distance between the two ends of the bent fiber at its relaxed position, $R(t)$, was taken as a measure of permanent deformation. The experiment was repeated using fresh, new fibers as a function of time from 10 to 240 min at temperatures close to and below the glass transition temperature, T_g, i.e., between 370 and 450°C. The T_g for the LS_2 and $LS_{1.6}$ glasses are $\sim 455 \pm 3$°C and $\sim 448 \pm 3$°C, respectively as determined by DTA at 10°C/min. Selected samples were coated with carbon using a Denton DV-515 Evaporator and examined in a Jeol T330A scanning electron microscope (SEM) operated at 20 or 25 kV.

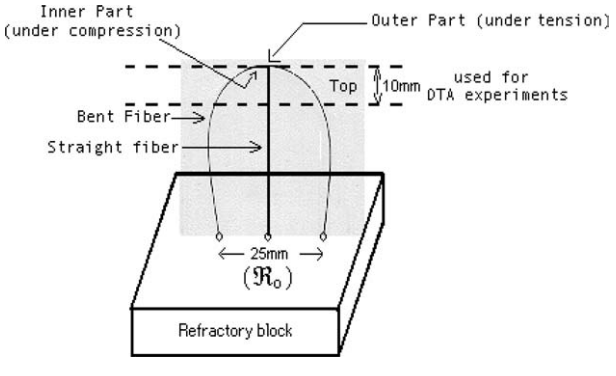

Figure 1 Schematic diagram of the glass fibers in a refractory block for heat treatment. Length of the glass fiber: 120 mm. Diameter of the glass fiber: 150 μm.

2.3. Analytical procedures for stress relaxation

2.3.1. Estimated bending stress

For a glass fiber bent in a circle of radius R_0, the bending stress (σ_0) at any point on the fiber is given by,

$$\sigma_0 = \frac{1.198 \cdot E \cdot d}{(R_0 - d)} \tag{2}$$

where E is the Young's modulus and d is the diameter of the glass fiber [11]. The diameter (d) of the glass fibers used in the present investigation was about 150 μm. The Young's modulii (E) for the LS_2 and $LS_{1.6}$ glasses are 80.3 and 81.6 GPa, respectively [13].

To estimate σ_0 at the tip of the bent glass fiber in the present configuration (Fig. 1), half of the distance, $\Re_0$, between the holes on the refractory block was approximated as the radius of curvature, R_0, in Equation 2. This assumption, however, introduces an error, since the configuration of the bent fiber is not exactly circular in the present case. Calculations show that this assumption overestimates the value of σ_0 by 30 to 40% [14]. Since the length of the fibers and the distance between the holes are always kept constant at 120 and 25 mm, respectively, the fibers for all the experiments will experience the same initial bending stress at the tip. Using the assumption $\Re_0/2 = R_0$, the value of σ_0 at the tip of the LS_2 and $LS_{1.6}$ glass fibers in the configuration shown in Fig. 1 is $\sim 1.16 \pm 0.01$ GPa.

2.3.2. Stress relaxation model

If a glass fiber while bent in a circular fashion with radius of curvature R_0 (bending stress σ_0, Equation 2) is released and allowed to relax after heat treating at T for a time t, it will take a circular shape with a radius of curvature, $R(t)$, which will be greater than R_0. If $\sigma(t)$ is the bending stress in the relaxed mode, the amount of relaxed stress, $\sigma_0 - \sigma(t)$, can be expressed in a single exponential form as [10],

$$\sigma_0 - \sigma(t) = \sigma_0 \exp(-t/\tau) \tag{3}$$

$$\text{or,} \quad 1 - \Psi(t) = \exp(-t/\tau) \tag{4}$$

where τ is the stress relaxation time and $\psi(t) = \sigma(t)/\sigma_0 \approx R_0/R(t)$ (for $d \ll R_0$ or $R(t)$) is the stress relaxation function. By definition, τ is the time at which the stress decreases to 63% of its initial value (σ_0).

Fig. 2 shows the typical shape of the deformed LS_2 or $LS_{1.6}$ glass fibers after heating at 390°C for the times shown. These pictures were taken on a scanner after placing the relaxed, heat treated glass fibers (coated with black ink) on a white paper. The distance between the two ends of the deformed fiber (after heat treatment for a time, t) is designated as $\Re(t)$, see Fig. 2. Thus, for the present analytical treatment, assuming, as before, $R(t) = \Re(t)/2$ and $2d \ll \Re(t)$ (Equation 2), the stress relaxation function for the glass fibers can be expressed as,

$$\Psi(t) = \sigma(t)/\sigma_0 = R_0/R(t) = \Re_0/\Re(t) \tag{5}$$

Plotting $\psi(t)$ as a function of t from the measured $\Re(t)$ and $\Re_0 (= 25$ mm) at different temperatures the values of $\tau(T)$ at different temperatures can be determined. The temperature dependence of τ can also be expressed in an Arrehenian form as,

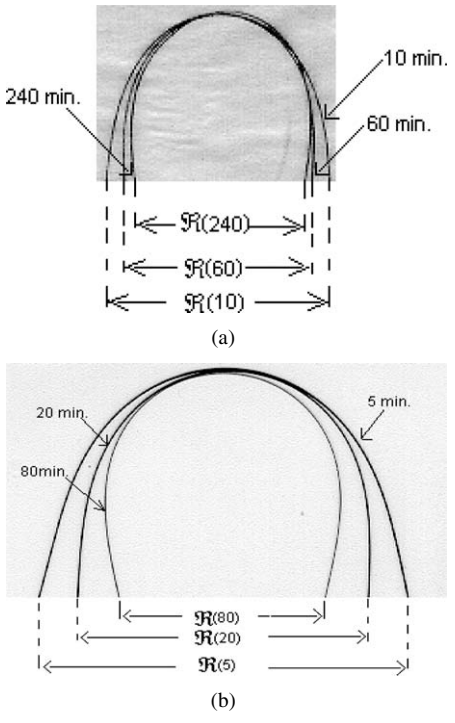

Figure 2 (a) Picture taken in a scanner for the LS_2 glass fibers after heating while bent at 390°C for 10, 60 or 240 min. The fibers were coated with black ink for improve the contrast. (b) Picture taken in a scanner for the $LS_{1.6}$ glass fibers after heating while bent at 390°C for 5, 20 or 80 min. The fibers were coated with black ink for improve the contrast.

$$\tau(T) = \tau_0 \exp\left(E_s/RT\right) \tag{6}$$

$$\ln \tau(T) = \ln \tau_0 + E_s/RT \tag{7}$$

where, E_s is the activation energy for stress relaxation, τ_0 is a pre-exponential factor, and R is the gas constant.

As will be shown later, the single exponential model cannot adequately describe the stress relaxation for the glass fibers in the present work. Thus, a stretched exponential decay model (Kohlrausch-Williams-Watts or KWW approximation) [15], as shown below, was used to fit the experimental results,

$$1 - \Psi(t) = \exp[(-t/\tau)^n], \quad 0 < n < 1 \tag{8}$$

The KWW approximation assumes that the stress relaxation proceeds through a series, instead of one, of exponential decay forms with several relaxation times. The relaxation times have a statistical distribution, and n in Equation 8 is the distribution parameter for relaxation times. A larger value for n signifies a narrower distribution of the relaxation times such that $n = 1$ defines a unique relaxation time, and the relaxation follows a single exponential law as shown in Equation 4. Conversely, a smaller value for n indicates a diffuse or wider distribution of relaxation times.

Equation 8 can be written as,

$$\log[-\ln(1 - \Psi(t))] = n \cdot \log(t/\tau) \tag{9}$$

Thus by plotting $\log[-\ln(1-\Psi(t))]$ against $\log(t/\tau)$, the value of n can be determined.

3. Results and discussion

3.1. Stress induced crystallization—Evidence of shear thinning

In the present experimental configuration (Fig. 1), the bent LS_2 glass fibers showed evidence of crystallization in the region of maximum bending stress (tip of the bent part) when heated at a temperature as low as 420°C, which is about 35°C lower than the glass transition temperature (T_g) and about 150°C lower than the onset temperature for crystallization (T_c) for this glass held at normal (stress-free) condition. The extent of crystallization increases with increasing heat treatment temperature. A typical example of crystallization for a bent LS_2 glass fiber when heated at 450°C (∼5°C less than T_g and 120°C less than T_c) for 12 h is shown in Fig. 3. Also shown in Fig. 3, for comparison, is an SEM image from a straight fiber (no stress) heated simultaneously with the bent fiber, which showed no evidence of crystallization.

Similar low temperature crystallization was also observed for the $LS_{1.6}$ glass fibers when heated under a bending stress. Fig. 4 shows the SEM pictures for portions of the bent (high stress) and straight (no stress) $LS_{1.6}$ glass fibers that were heated at 410°C (∼ 38°C less than T_g and 150°C less than T_C) for 12 h. While the bent fiber clearly shows evidence of crystallization, the straight fiber still appears to be a homogeneous glass. These results for the LS_2 and $LS_{1.6}$ glass fibers clearly demonstrate that the crystallization temperature is decreased by more than 150°C when the glass fibers are subjected to a bending stress of ∼1.2 GPa, compared to that for the stress-free glass fibers.

Under a bending mode, the inner part of the glass fiber should be under compression, and the outer part should be under tension (Fig. 1). No difference in the extent of crystallization between the inner and outer regions of the glass fiber was evident (compare Fig. 3c and d or Fig. 4c and d which suggests that the compressive and tensile stresses have nearly the same effect on crystallization.

There was a central region, almost parallel to the axis of the glass fiber, where there was either no evidence of crystallization or the extent of crystallization was small compared to the extent of crystallization at the inner and outer regions of the bent fiber (for example see Fig. 3a). The applied stress in the central region of these fibers is expected to be minimum.

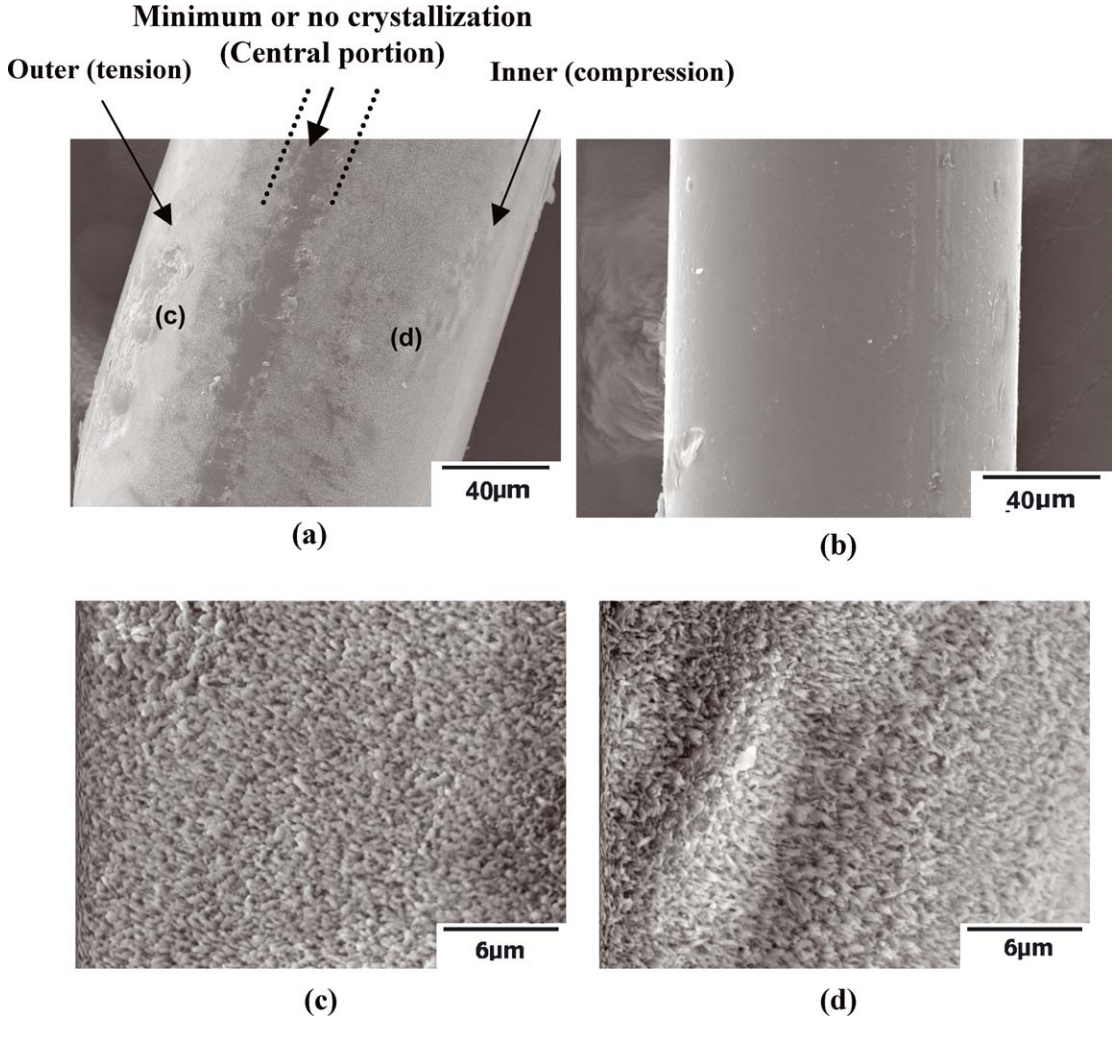

Figure 3 Scanning electron microscope pictures of the (a) stressed and (b) un-stressed (straight) LS_2 glass fibers after heating at 450°C for 12 h. (c) and (d) are the enlarged view of the outer and inner part of stressed fiber at locations shown in (a). No crystallization is observed on the heat treated straight fiber (b).

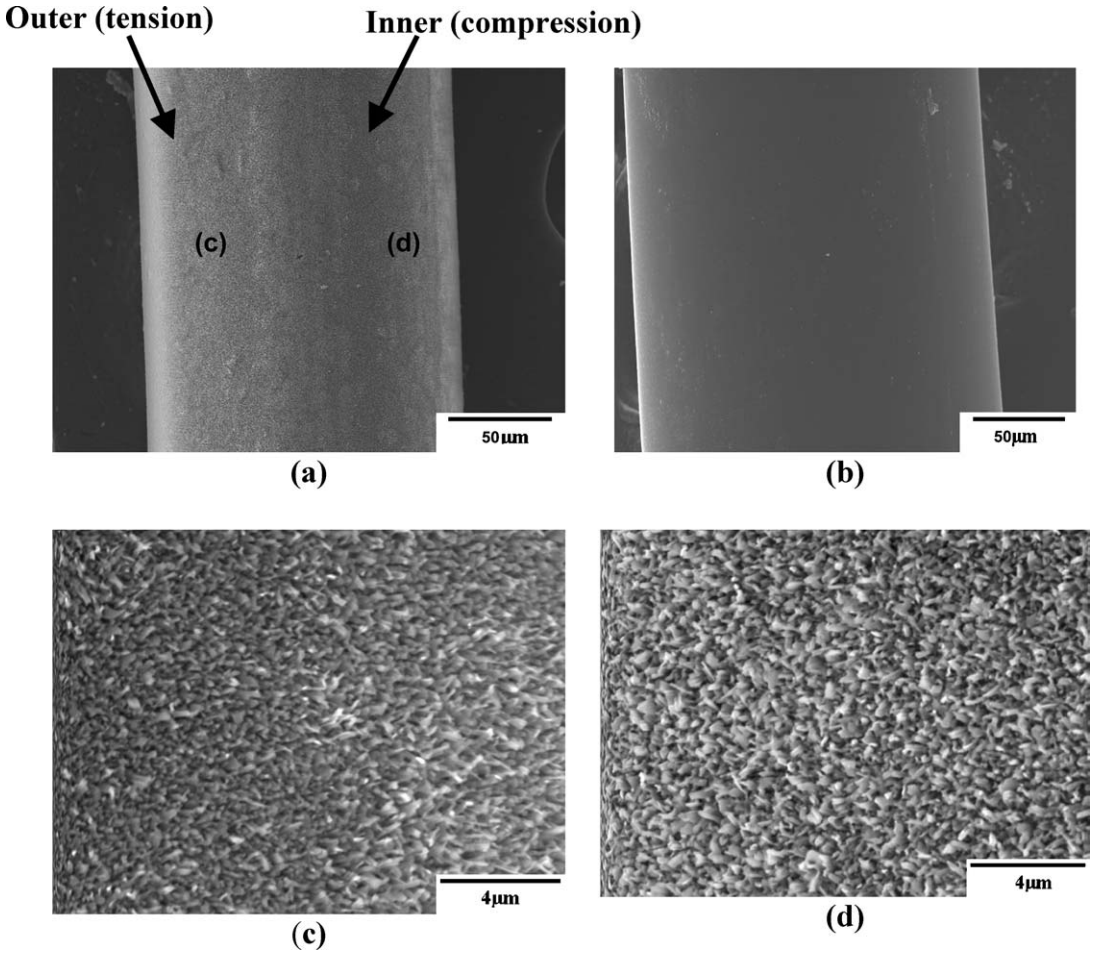

Figure 4 Scanning electron microscope pictures of the (a) stressed and (b) un-stressed (straight) $LS_{1.6}$ glass fibers after heating at 410°C for 12 h. (c) and (d) are the enlarged view of the outer and inner part of stressed fiber at locations shown in (a). No crystallization is observed on the heat treated straight fiber (b).

3.2. Deformation of glass fibers and stress relaxation

3.2.1. Relaxation time (τ) and activation energy for stress relaxation (E_S)

The dependence of the stress relaxation function, $\psi(t)$ (Equation 5), on the heat treatment time, t, at different temperatures is shown in Fig. 5 for the LS_2 glass fibers and in Fig. 6 for the $LS_{1.6}$ glass fibers. The conventional procedure [11, 12] for determining the values for relaxation time, τ, was followed, i.e., the time corresponding to the intersection of the curves in Figs 5 and 6 with the horizontal line for $\psi(t) = 0.63$ (Equation 4) was taken as a measure of τ (indicated by dashed lines in Figs 5 and 6). The measured value of τ at any temperature for the LS_2 glass fibers is higher than that of the $LS_{1.6}$ glass fibers, see Fig. 7. The difference in τ-values for the LS_2 and $LS_{1.6}$ glass fibers is more pronounced in the low temperature region, and becomes almost indistinguishable as T_g is approached.

The values of τ determined from Figs 5 and 6, and shown in Fig. 7 at different temperatures were plotted as a function of the reciprocal of temperature in Fig. 8 for the LS_2 and $LS_{1.6}$ glass fibers. In accordance with Equation 7, the data points in Fig. 8 for both glass fibers fit a linear regression very well with a correlation factor of better than 0.998. The slope of the straight lines in Fig. 8 is the activation energy for stress relaxation, E_s, which is about 194±5 kJ/mol and 175±5 kJ/mol for the LS_2 and $LS_{1.6}$ glass fibers, respectively. Although this difference in E_s is not very high, a higher value of E_s for the LS_2 glass fibers may indicate a higher resistance to stress relaxation compared to that for the $LS_{1.6}$ glass fibers, which is also evident from higher values of τ for the LS_2 glass fibers at all temperatures (Fig. 7).

The values of E_s and the pre-exponential factor, τ_0, for the present LS_2 and $LS_{1.6}$ glass fibers are listed in Table I along with the reported values of E_s and τ_0 for a several optical glass fibers [11]. Koide *et al.* [11, 12] suspect that deformation in the SiO_2 glass fibers is caused mainly by a free volume reduction. While the free volume reduction may contribute to the deformation of LS_2 or $LS_{1.6}$ glass fibers observed in the present work, the migration of Li^+ ions might also contribute to the deformation of these fibers.

TABLE I Kinetic parameters, E_s, τ_o, and n for stress relaxation

Glass fiber	E_s (KJ/mol)	τ_o (h)	n (±0.02) (average)	Reference
SiO_2	202 ± 3	1.9×10^{-10}	0.49	[11]
LS_2	194 ± 5	1.1×10^{-14}	0.48	Present work
$LS_{1.6}$	175 ± 5	1.2×10^{-13}	0.43	Present work
F-doped SiO_2	145 ±3	1.2×10^{-7}	0.69	[11]
GeO_2-doped SiO_2	188 ± 3	4.3×10^{-10}	0.68	[11]
Fluoride glass fiber	144 ±3	4.5×10^{-17}	0.28	[11]

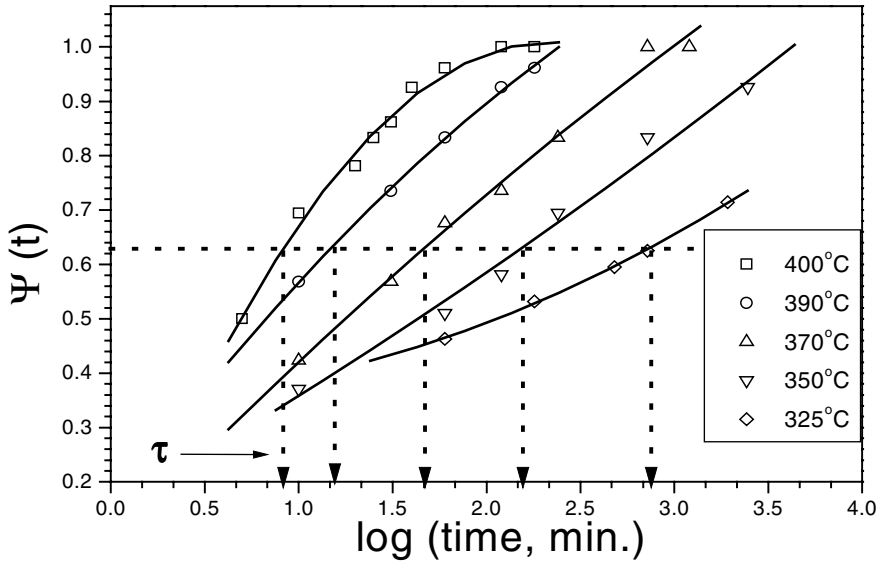

Figure 5 The relaxation function, $\Psi(t)$ for the LS_2 glass fibers as a function of heat treatment time for temperatures between 325 and 400°C. The glass transition temperature for the LS_2 glass is ∼455°C.

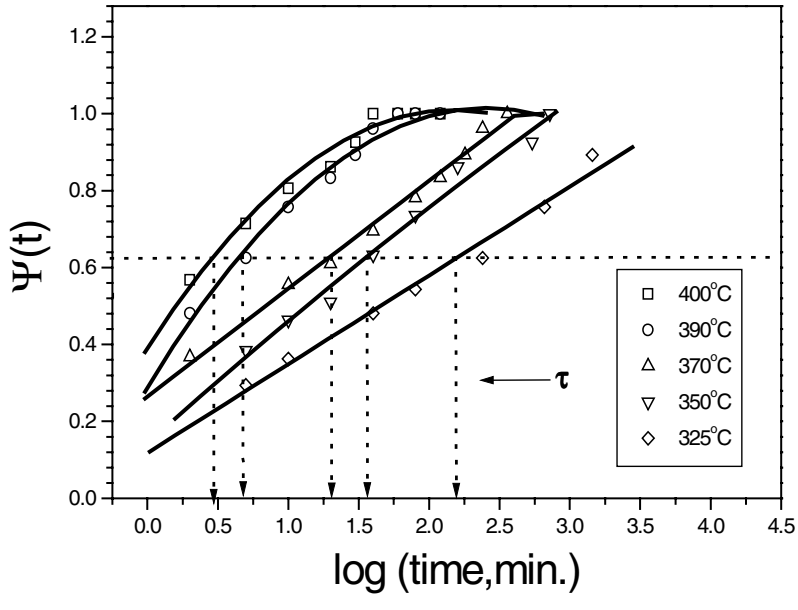

Figure 6 The relaxation function, $\Psi(t)$ for the $LS_{1.6}$ glass fibers as a function of heat treatment time for temperatures between 325 and 400°C. The glass transition temperature for the $LS_{1.6}$ glass is ∼448°C.

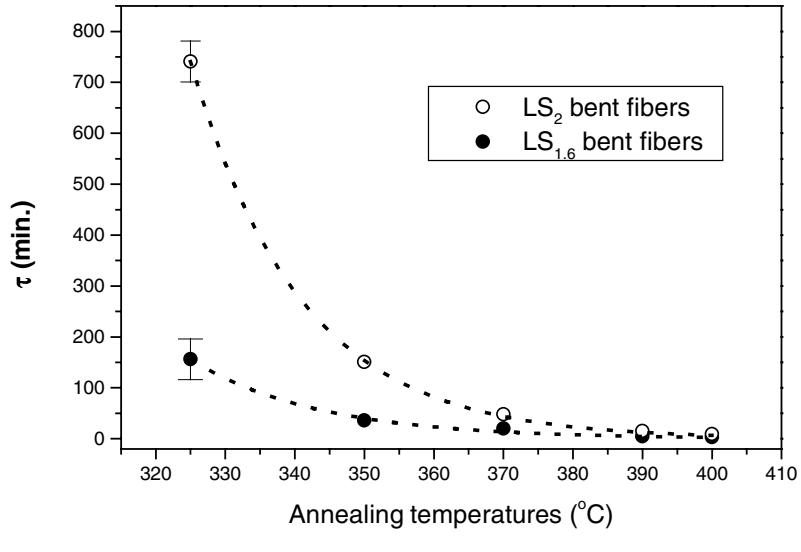

Figure 7 The relaxation time, τ, for the LS_2 and $LS_{1.6}$ glass fibers at temperatures between 325 and 400°C. Estimated experimental error is shown on one data point for each type of fibers.

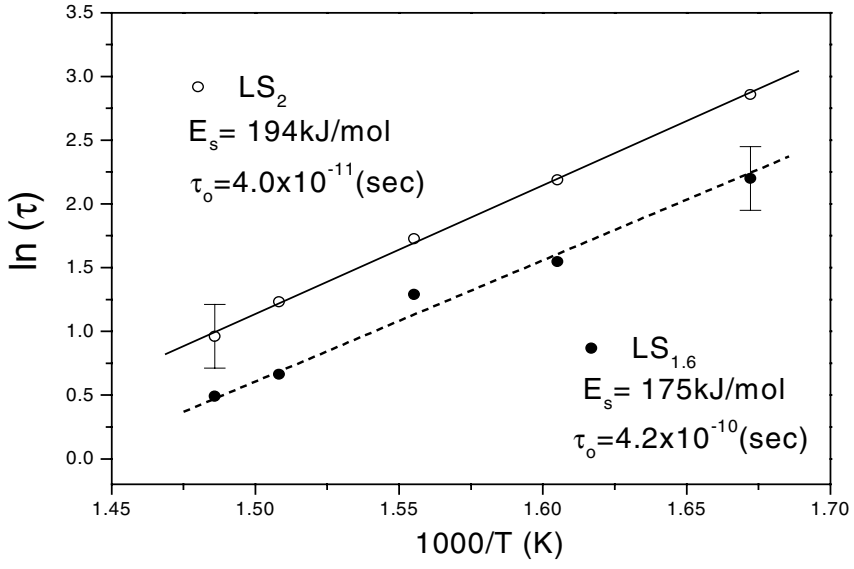

Figure 8 Plot of $\ln\tau$ vs. $1/T$ for the LS_2 and $LS_{1.6}$ glass fibers, see Equation 7.

3.2.2. Distribution parameter for relaxation time, n (stretched exponential or KWW approximation)

The experimental data for the stress distribution function (ψ) from the present work did not exactly fit the single exponential curve generated using the measured relaxation time, τ. An example is shown in Fig. 9, where the values of $[1-\psi(t)]$ for the LS_2 glass fiber are shown as a function of heat treatment time at 390°C. These results for ψ were then re-plotted according to Equation 9 (KWW model) and are shown in Figs 10 and 11 for the LS_2 and $LS_{1.6}$ glass fibers, respectively. The data points for both glass fibers (Figs 10 and 11) generally fit a straight line, although some random scatter in the data points is apparent. The scatter in the data points arises primarily because of the fact that the values of ψ from all the experiments at different temperatures for either the LS_2 or $LS_{1.6}$ glass fibers are included in Fig. 10 or 11.

The slope of the straight line in Fig. 10 or 11 gives, according to Equation 9, an average value for the distribution parameter for relaxation time, n, which is about 0.48 for the LS_2 glass fibers and about 0.43 for the $LS_{1.6}$ glass fibers. The stretched exponential curve generated using this average n-value describes adequately the experimental data for both types of glass fibers; examples are shown in Figs 12 and 13 for the LS_2 and $LS_{1.6}$ glass fibers, respectively, when heated at 390°C for different times. The average n-value for the LS_2 and $LS_{1.6}$ glass fibers from the present experiments is given in Table I along with the reported n-value for a few other optical glass fibers for comparison [11]. Like the activation energy for stress relaxation (E_s), the n-values for the LS_2 and SiO_2 glass fibers are also similar. The pre-exponential factor, τ_0, is very different for different glass fibers listed in Table I.

The scatter in the data in Figs 10 and 11 was further investigated by plotting $\log[-\ln(1-\psi)]$ vs. $\log(t/\tau)$

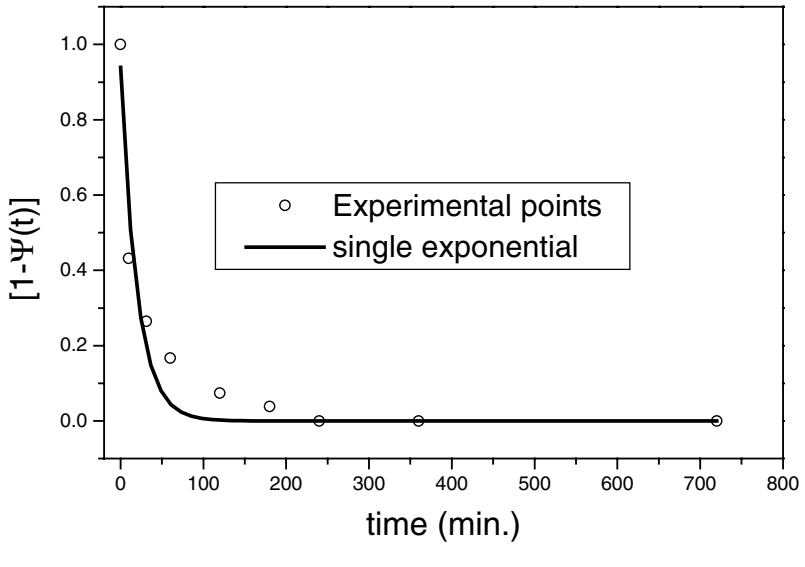

Figure 9 Plot of $[1-\Psi(t)]$ vs. time for the LS_2 glass fiber after heating at 390°C using a single exponential form. Not all the experimental data points fit this single exponential curve.

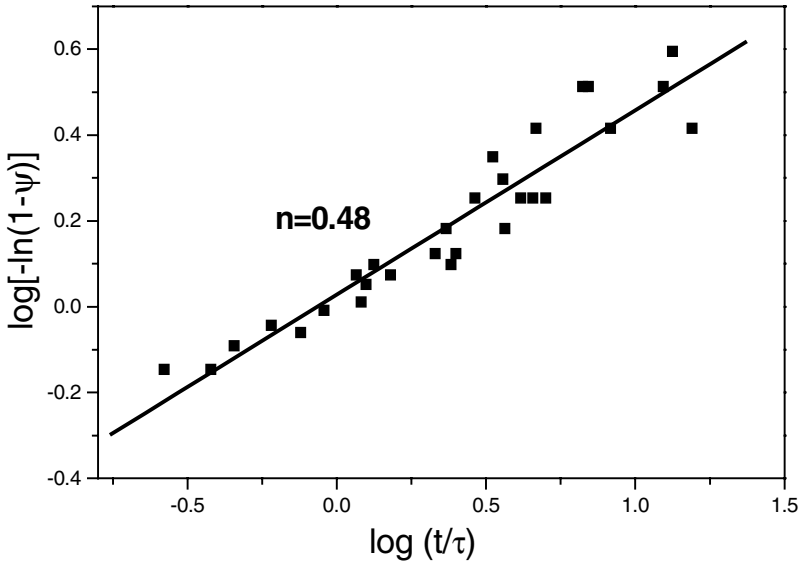

Figure 10 Plot of $\log[-\ln(1-\Psi)]$ vs. $\log(t/\tau)$ for the LS_2 glass fibers, see Equation 9.

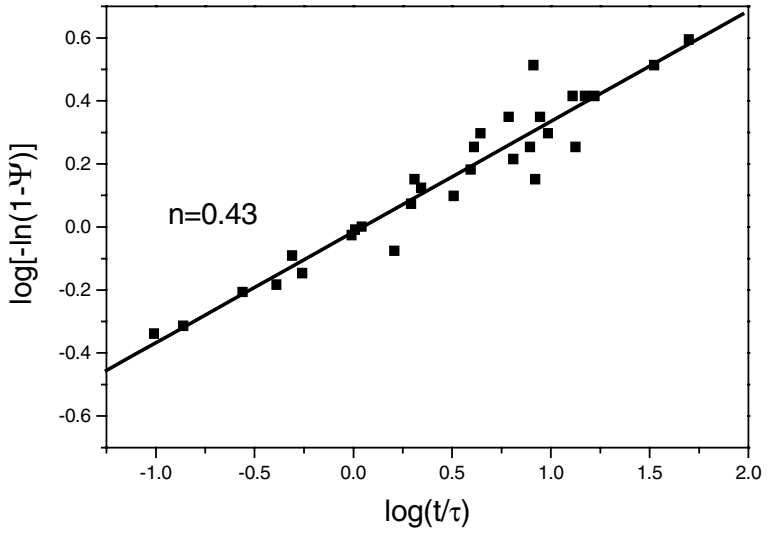

Figure 11 Plot of $\log[-\ln(1-\Psi)]$ vs. $\log(t/\tau)$ for the $LS_{1.6}$ glass fibers, see Equation 9.

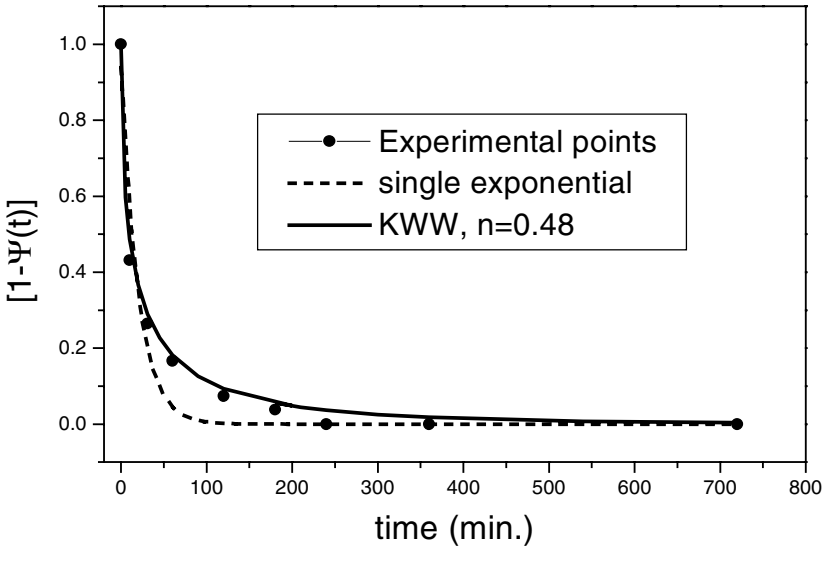

Figure 12 Plot of $[1-\Psi(t)]$ vs. time for the LS_2 glass fiber after heating at 390°C, using a single or a stretched (KWW) exponential form. The experimental data points are described better by the stretched exponential form.

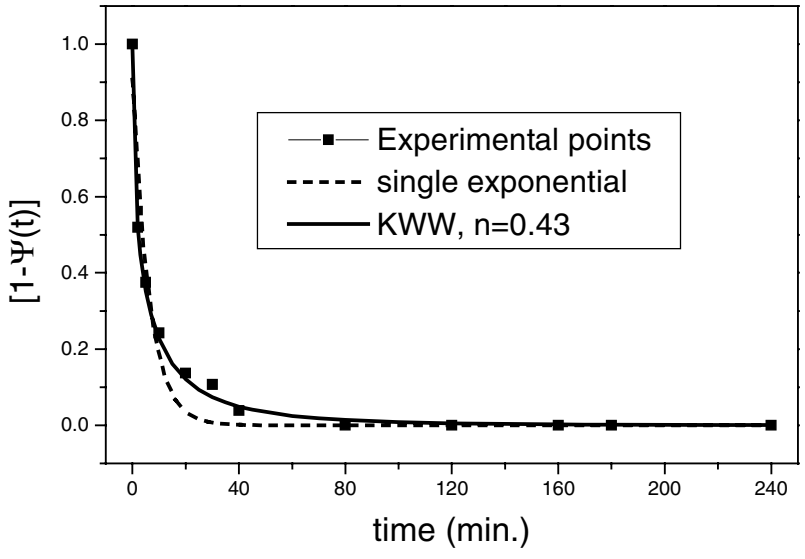

Figure 13 Plot of $[1 - \Psi(t)]$ vs. time for the $LS_{1.6}$ glass fiber after heating at 390°C, using a single or a stretched (KWW) exponential form. The experimental data points are described better by the stretched exponential form.

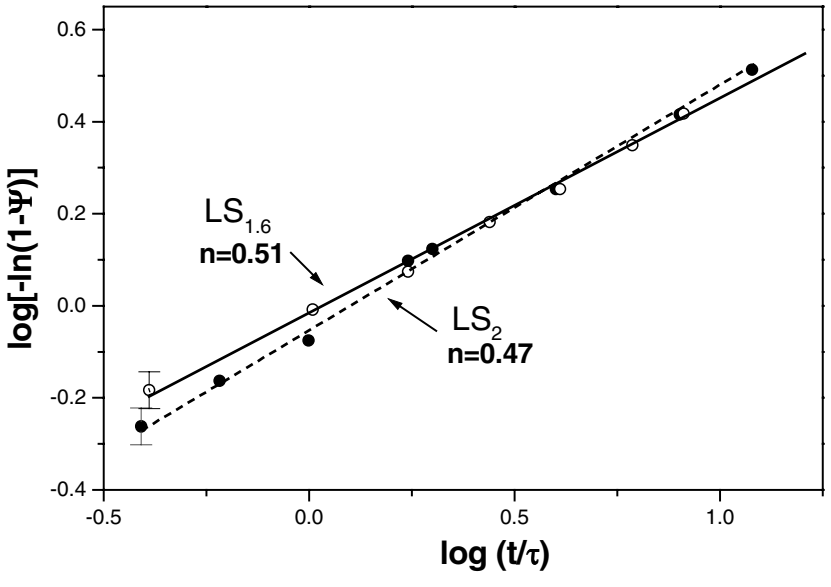

Figure 14 Plot of $\log[-\ln(1 - \Psi)]$ vs. $\log(t/\tau)$ for the LS_2 and $LS_{1.6}$ glass fibers at 390°C. The experimental data points fit the linear regression very well.

separately for each temperature, and the data points fit a linear regression nicely in each case, see Fig. 14 as an example at 390°C. The n-values determined from the slope of each straight line, such as those shown in Fig. 14, are shown in Fig. 15 as a function of temperature for the LS_2 and $LS_{1.6}$ glass fibers. Fig. 15 clearly shows that the distribution parameter (n) for relaxation time is, at least for the present LS_2 and $LS_{1.6}$ glass fibers, temperature dependent and increases with increasing temperature, i.e., the distribution of relaxation time becomes narrower (approaches to single exponential) as the temperature increases. Similar temperature dependence of n for the SiO_2 glass fibers has also been reported [11].

Like what was observed [11] for the activation energy for stress relaxation (E_s) for the SiO_2 glass fibers, the E_s for the LS_2 and $LS_{1.6}$ glass fibers was much smaller than the activation energy for viscous flow ($E_\eta \sim 400$ to 450 kJ/mol) for these glasses [11, 12]. For this reason, it was concluded [11] that the deformation mechanism of the SiO_2 glass fibers below the glass transition temperature (T_g) was very different from the mechanism of viscous flow. Although this conclusion seems reasonable, the important factor for the change of viscosity with time at any temperature or viscosity relaxation mechanism has not been taken into consideration. As mentioned by Doremus [16], the activation energy for viscosity relaxation, $E_{\eta r}$, for glasses, especially silicate glasses, is much less than the activation energy for viscous flow, E_η, typically, $E_{\eta r} \approx 1/2E_\eta$. For example, $E_{\eta r}$ for a soda-lime-silica glass was reported to be about 400 kJ/mol, where as, E_η for the same glass in the high viscosity region is about 718 kJ/mol [16]. The activation energy for stress relaxation (E_s) determined for the LS_2 and $LS_{1.6}$ glass fibers in the present investigation is believed to be comparable with the activation energy for viscosity relaxation for these glasses in the high viscosity (low temperature) region. In other

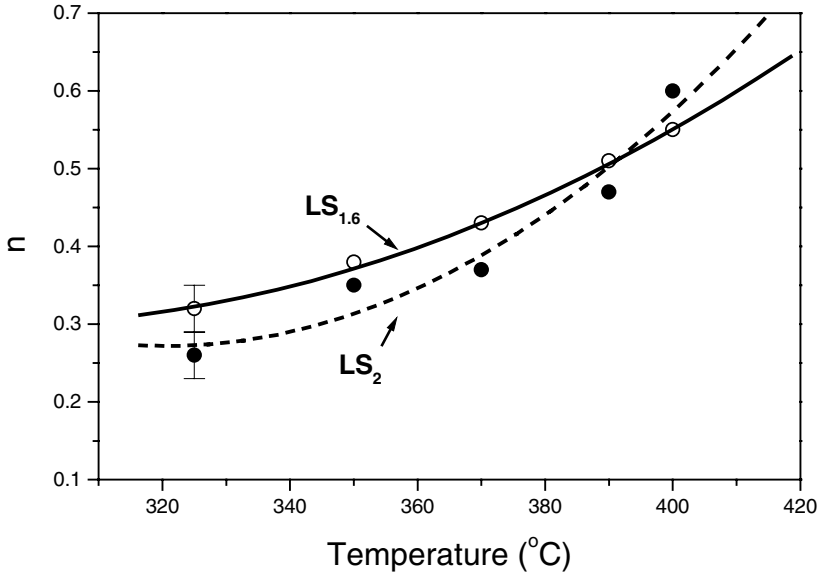

Figure 15 Temperature dependence of the distribution parameter for relaxation time, n, for the $LS_{1.6}$ and LS_2 glass fibers.

words, stress relaxation mechanism in these glass fibers appears to be related to the mechanism of viscosity oscillation.

An increasing tendency for crystallization, at least surface crystallization, with increasing bending stress was unambiguously demonstrated for these glass fibers, the reason for which, however, is not clearly understood at this time. Several possible factors, occurring either separately or concurrently, may be responsible for this result. The effect of shear thinning, a decrease in viscosity with the applied bending stress, is believed to be the most likely reason for enhancing the tendency for crystallization. A structural organization under bending stress creating regions of increased Li^+ concentration may also be a likely reason. This factor, namely, structural organization, which should be augmented by viscous flow, can be a consequence of shear thinning. Another reason may be the possibility for developing micro-cracks on the surface of the glass fibers under a bending mode, which subsequently acted as potential sites for crystallization. Glasses below their glass transition temperatures are considered [17, 18] visco-elastic solids, i.e., they display both elastic and viscous properties. Viscous relaxation and elastic stress relaxation are reported [18, 19] to have opposing effects on the driving force for forming the critical clusters and, hence, on crystallization of the glass. However, how these relaxation processes are affecting the formation of critical clusters leading to an increase in the overall tendency for crystallization of the glass fibers under a bending stress in the present study is not known, and will be the subject of a future study.

4. Conclusions

The crystallization tendency of the LS_2 and $LS_{1.6}$ glass fibers at any temperature is enhanced when these glass fibers are subjected to a bending stress. Under a bending stress, these glass fibers crystallize at temperatures that are 35 to 40°C lower than the glass transition temperature (T_g) or more than 150°C lower than the onset temperature for crystallization for these glasses in normal (stress-free) conditions. No crystallization was observed when the same glass fibers, under stress-free condition, were heated at these temperatures. An effect of shear thinning caused by the bending stress is suspected to be the reason for the observed increase in the tendency for crystallization, although other factors, such as, structural organization of the glass network, development of micro-cracks on the surface of the glass fibers, and a decrease in the driving force for forming critical clusters due to viscosity relaxation cannot be totally ruled out.

The stress relaxation process of the glass fibers is described better by a stretch exponential, rather than a single exponential, mechanism with an average distribution parameter (n) for the relaxation time between 0.45 and 0.48, and activation energy for stress relaxation (E_s) between 175 and 200 kJ/mol. The values of E_s and n for the LS_2 and $LS_{1.6}$ glass fibers are comparable with those for a SiO_2 glass fiber.These values of E_s are smaller than the activation energy for viscous flow, but are believed to be comparable with the activation energy for viscosity relaxation.

The effect of bending stress on deformation and crystallization is more pronounced in the $LS_{1.6}$ than in the LS_2 glass fibers. This is most likely due to the reason that the $LS_{1.6}$ glass contains a higher concentration of the more mobile Li^+ ions. A higher concentration of Li^+ ions establishes larger viscous flow (or larger amplitude for viscosity relaxation) in the $LS_{1.6}$ glass fiber under the stress causing its deformation and crystallization tendencies to increase, and stress relaxation time (τ) to decrease at all temperatures compared to those for an LS_2 glass. Since, the $LS_{1.6}$ glass has a higher de-polymerized network structure than the LS_2 glass, it appears that a glass with a higher degree of network de-polymerization is more susceptible to shear thinning, deformation, and crystallization.

Acknowledgements

This work was supported by the University of Missouri Research Board. The authors are grateful to Dr. Delbert E. Day for many helpful discussion and suggestions. One of the authors, S. T. Reis, highly appreciates the support from the University of Missouri Rolla, which has made this work possible.

References

1. J. H. SIMMONS, R. K. MOHR and C. J. MONTROSE, *J. Appl. Phys*. **53** (1982) 4075.
2. J. M. JACOBS, "Newtonian and Non-Newtonian Viscous Flow Behavior in Various Commercial Glass Compositions," MS Thesis, Alfred University, Alfred, New York, 1999.
3. J. H. LI and D. R. UHLMANN, *J. Non-Cryst. Solids* **3** (1970) 127.
4. G. H. BEALL and C. J. QUINN, "Zinc Containing Phosphate Glasses," US Patent 4940677, July 1990.
5. C. E. CROWDER, J. U. OTAIGBE, M. A. BARGER, R. L. SAMMLER, B. C. MONAHAN and C. J. QUINN, *J. Non-Cryst. Solids* **210** (1997) 209.
6. I. GUTZOW, A. DOBREVA and J. SCHMELZER, *J. Mater. Sci*. **28** (1993) 890.
7. *Idem*., *ibid*. **28** (1993) 901.
8. J. DEUBENER and R. BRUCKNER, *J. Non-Cryst. Solids* **209** (1997) 96.
9. V. I. ARBUZOV, G. CARL, C. RUSSELL and B. DURSCHANG, *Glasstechn. Berichte: Glass Sci. Techn*. **71** (1998) 277.
10. D. R. UHLMANN and H. YINNON, "The Formation of Glasses: Glass Science and Technology", edited by D. R. Uhlman and N. J. Kreidl (Academic Press, New York, 1983) Vol. 1, p. 1.
11. M. KOIDE, R. SATO, T. KOMATSU and K. MATUSITA, *J. Non-Cryst. Solids* **177** (1994) 427.
12. *Idem.*, *Phys. Chem. Glasses* **38** (1997) 83.
13. A. MAKISHIMA and J. D. MACKENZIE, *J. Non-Cryst. Solids* **12** (1973) 35.
14. M. M. MATTHEWSON and C. R. KURKJIAN, *J. Amer. Ceram. Soc*. **11** (1986) 815.
15. G. W. SCHERER, "Glass Formation and Relaxation: Materials Science and Technology", edited by R. W. Cahn, P. Haasen and E. J. Kramer (Glasses and Amorphous Materials), volume editor, J. Zarzycki (VCH Publications, New York, NY, 1991) Vol. 9, p. 120.
16. R. H. DOREMUS, *Amer. Ceram. Soc. Bull.* **82** (2003) 59.
17. I. GUTZOW and J. SCHMELZER, "The Vitreous State: Thermodynamics, Structure, Rheology, and Crystallization" (Springer, Berlin, 1999).
18. J. W. P. SCHMELZER, R. MÜLLER, J. MÖLLER and I. S. GUTZOW, *J. Non-Cryst. Solids* **315** (2003) 144.
19. J. W. P. SCHMELZER, O. V. POTAPOV, V. M. FOKIN, R. MÜLLER and S. REINSCH, *ibid.* **333** (2004) 150.

Received 18 June 2003
and accepted 3 June 2004